TRANSPLANT INTERNATIONAL

Transplant International ISSN 0934-0874

ORIGINAL ARTICLE

Decreased expression of mitochondrial aldehyde dehydrogenase-2 induces liver injury via activation of the mitogen-activated protein kinase pathway

Zibiao Zhong,[1] Shaojun Ye,[1] Yan Xiong,[1] Lianxi Wu,[4] Meng Zhang,[1] Xiaoli Fan,[1] Ling Li,[1] Zhen Fu,[2] Huanglei Wang,[1] Mingyun Chen,[1] Xiaomin Yan,[1] Wei Huang,[1] Dicken Shiu-Chung Ko,[3] Yanfeng Wang[1] and Qifa Ye[1,2]

1 Wuhan University, Zhongnan Hospital of Wuhan University, Institute of Hepatobiliary Diseases of Wuhan University, Transplant Center of Wuhan University, Hubei Key Laboratory of Medical Technology on Transplantation, Wuhan Hubei, China
2 The 3rd Xiangya Hospital of Central South University, Research Center of National Health Ministry on Transplantation Medicine Engineering and Technology, Changsha, China
3 Massachusetts General Hospital, Department of Urology, Harvard Medical School, Boston, MA, USA
4 Jianghan District Center for Disease Control and Prevention, Wuhan Hubei, China

Keywords
apoptosis, brain death, mitochondrial aldehyde dehydrogenase 2, mitogen-activated protein kinase pathway.

Correspondence
Qifa Ye, MD, Donghu Road, NO 169, Institute of Hepatobiliary Diseases, Zhongnan Hospital of Wuhan University, Wuhan 430071, China.
Tel.: 86-13875987051;
fax: 86-027-67812988;
e-mail: yqf_china@163.com

Yanfeng Wang, MD, Donghu Road NO 169, Institute of Hepatobiliary Diseases, Zhongnan Hospital of Wuhan University, Wuhan, 430071, China
Tel: 86-15392891693
fax: 86-027-67812988
Email: yanfengwang@whu.edu.cn

Conflicts of interest
The authors have declared that no conflict of interests in the manuscript.

Received: 12 February 2015
Revision requested: 31 March 2015
Accepted: 20 August 2015
Published online: 25 September 2015

doi:10.1111/tri.12675

Summary

The aim of this study was to determine the role of ALDH2 in the injury of liver from brain-dead donors. Using brain-dead rabbit model and hypoxia model, levels of ALDH2 and apoptosis in tissues and cell lines were determined by Western blot, flow cytometry (FCM), and transferase (TdT)-mediated biotin-16-dUTP nick-end labeling (TUNEL) assays. After the expression of ALDH2 during hypoxia had been inhibited or activated, the accumulations of 4-hydroxynonenal (4-HNE) and molecules involved in mitogen-activated protein kinase (MAPK) signaling pathway were analyzed using ELISA kit and Western blot. The low expression of phosphorylated ALDH2 in liver was time-dependent in the brain-dead rabbit model. Immunohistochemistry showed ALDH2 was primarily located in endothelial, and the rates of cell apoptosis in the donation after brain-death (DBD) rabbit groups significantly increased with time. Following the treatment of inhibitor of ALDH2, daidzein, in combination with hypoxia for 8 h, the apoptosis rate and the levels of 4-HNE, P-JNK, and cleaved caspase-3 significantly increased in contrast to that in hypoxic HUVECs; however, they all decreased after treatment with Alda-1 and hypoxia compared with that in hypoxic HUVECs ($P < 0.05$). Instead, the levels of P-P38, P-ERK, P-JNK, and cleaved caspase-3 decreased and the ratio of bcl-2/bax increased with ad-ALDH2 (10^6pfu/ml) in combination with hypoxia for 8 h, which significantly alleviated in contrast to that in hypoxic HUVECs. We found low expression of ALDH2 and high rates of apoptosis in the livers of brain-dead donor rabbits. Furthermore, decreased ALDH2 led to apoptosis in HUVECs through MAPK pathway.

Introduction

Liver transplantation is the most effective treatment for end-stage liver diseases; however, the availability of donor organs limits the availability of liver transplants [1]. In China, a growing number of liver allografts are now available from donors after brain death (DBD) [2–5]. Nevertheless, immediate and long-term morbidity and mortality of

recipients of DBD donor livers are relatively poor when compared with living donors [6,7]. Several studies have revealed that these DBD livers of newly transplanted are associated with hepatocyte apoptosis which may contribute to less ideal outcomes [8,9]. However, the factors that lead to hepatocyte apoptosis have yet to be determined, and there is an urgent need to determine the mechanism involved in DBD liver donors.

Some studies have implied that the currently used clinical indices could not evaluate the quality of liver donors [10,11]. Previously, we established a rabbit DBD model to study on the liver morphology and found no obvious changes at different time points. We subsequently utilized a proteomic assay to screen differentiated proteins in the liver in order to determine whether there are any differences notable in DBD livers. It has been published that aldehyde dehydrogenase 2 (ALDH2) was shown to be significantly lower in DBD liver donors [12,13]. However, few studies have focused on the relationships between ALDH2 and DBD liver donors.

Human ALDH2 is encoded by a nuclear gene located at chromosome 12q24, and the protein is transported to the mitochondrial matrix. It is known that aldehydes are major contributors to the pathology of lots of human diseases, while more data strongly support an important protection role for the ubiquitous mitochondrial ALDH2. Moreover, ALDH2 is an antioxidant stress protection factor, which mainly not only refers to exogenous lipids, aromatic aldehyde metabolism, and detoxification, but also degrades highly toxic aldehydes (the highly toxic aldehyde is mainly 4-HNE) originating from the lipid peroxidation cascade [14]. Previous reports have suggested that ethanol stimulates expression of ALDH2 and increases expression of phosphorylated Akt and Pim as a result, while hepatocyte apoptosis is decreased [15]. In contrast, acetaldehyde mediates the production of oxygen-free radicals, which is associated with apoptosis [16]. The upregulation of ALDH2 decreases extracellular signaling regulation of kinase 1/2 (EPK1/2) and p38 protein kinase, and the inhibition of apoptosis plays a role in cell protection [17]. In view of this, we speculate that the overexpression of ALDH2 alleviates cell apoptosis and protects the cells.

The mitogen-activated protein kinase (MAPK) family has an important effect on regulating inner cell signaling transduction. MAPK is comprised of three subfamilies (extracellular signaling regulation kinase [ERK], c-Jun N-terminal kinase [JNK], and p38 protein kinase). Previous researches have shown that the overexpression of ALDH2 decreases the expression of ERK1/2 and SPAK/JNK, thus preventing aldehydes from destroying cardiac and lung cells by limiting the expression of inflammatory factor AP-1 [15,18]. Low ALDH2 levels result in the accumulation of 4-HNE, and then, 4-HNE can activate the MAPK pathway [19], which may be involved in the process of brain-death-related liver injury. In this study, we have determined that mitochondrial ALDH2 levels are related to the pathway of apoptosis and clarified the mechanisms underlying liver injury resulting from brain death.

Materials and methods

Animals and grouping

Sixty healthy male rabbits (12 weeks old, weighing 2.9 ± 0.3 kg) were obtained from the Wan Qian Jia He Experimental Animal Culture Center (Wuhan, China) and equally divided into two groups (n = 30). All animal experiments were carried out in accordance with the Experimental Animal Regulations of the People's Republic of China and the Guide for the Care and Use of Laboratory Animals of the USA. The samples were collected at 2, 6, and 8 h after brain death or sham. Hence, each group was further divided into DBD 2, 6, and 8 h and sham 2, 6, and 8 h groups (n = 10).

Development of brain-death model

The criteria of brain death were in accordance with the USA Adult Brain Death Diagnostics Guide [20], as follows: (i) no pupillary or corneal reflex to light (two times); (ii) no spontaneous respirations; and (iii) no electroencephalographic activity. Briefly, the procedures of establishing brain-death models were as follows. Before surgery, the rabbits were weighed, skin was preserved, and anesthesia was administered. Tracheal intubation was used with a Y-shaped tube. The respirator was also prepared for use. The respiratory wave was monitored by contact with the ensisternum. Electroencephalography and electrocardiography were also performed. The body temperature was maintained at 38 °C by an intelligent temperature controller (Taimeng Biological Technology Co. LTD, Chengdu, China). Saline was injected through a catheter in the middle of the calva until the end of spontaneous respirations. Then, tracheal intubation was linked to a microrespirator and index changes were monitored. Dopamine (2 μg/kg/min) was used to maintain stable pressure by intravenous injection (iv). In the sham group, rabbits were catheterized without pressure; the other procedures were the same as the DBD group.

Culturing human umbilical vein endothelial cells (HUVECs) and grouping

HUVECs were obtained from American Type Culture Collection (ATCC; Manassas, VA, USA) and cultured in DMED medium with 10% fetal bovine serum (FBS) in a

humidified atmosphere with 5% CO_2 at 37 °C. The cultured cells were divided into four groups, as follows: group 1, the cells were cultured in normal conditions with 5% CO_2 at 37 °C; group 2, hypoxic conditions with 95% N_2+5% CO_2 for 8 h; group 3, incubation with daidzein (60 μM) in normal conditions for 24 h, and further culture under the same conditions in group 2 [21]; and group 4, the culture medium contained Alda-1 (20 μM), the cells were treated for 1 h [22], and those cells were also cultured under the same conditions in group 2. To further study on the relationship between ALDH2 and apoptosis, the cultured cells were further divided into four groups, as follows: group 5, the cells were cultured in normal conditions with 5% CO2 at 37 °C; group 6, hypoxic conditions with 95% N2 + 5% CO2 for 8 h; group 7, incubation with adenovirus empty vector (10^6pfu/ml) in normal conditions for 24 h and further culture under the same conditions in group 6; and group 8, incubation with ad-ALDH2 (10^6pfu/ml) in normal conditions for 24 h and further culture under the same conditions in group 6.

Western blot

After protein extraction from mitochondria, the concentration was determined. Then, sodium dodecyl sulfate–polyacrylamide gel electrophoresis transferred, soaked, and incubated with primary anti-ALDH2 (1:200 dilution; Huata Biological Technology Co., LTD, Guangzhou, Guangdong, China), anti-caspase-3 (1:1000; Biogood Technology, Inc, Wuhan, Hubei, China), anti-bax (1:100; Beijing Biosynthesis Biotechnology CO.LTD, Beijing, China), anti-bcl-2 (1:100; Beijing Biosynthesis Biotechnology CO.LTD), anti-ERK1/2 (1:2000; Bioworld Technology, Inc, Nanjing, Jiangsu, China), anti-phospho-ERK1/2 (1:1000; Cell Signaling Technology, Shanghai, China), anti-JNK (1:2000; Abcam Plc, Cambridge, England), anti-phospho-JNK (1:1000, Santa Cruz Biotechnology, Inc, Dallas, CA, USA), anti-p38 (1:2000; Epicentre, Madison, WI, USA), anti-phospho-p38 (1:1000; CST), and anti-β-actin (1:10 000; Santa Cruz Biotechnology, Inc) antibodies at 4 °C overnight. The proteins were detected using a luminescence method [ECL Western blotting detection with IgG antibodies, respectively, (1:5000) dilution]. The β-actin was used as the loading control.

Immunohistochemical testing

The fixed tissues were washed with PBS and vibratome-sectioned into 60- to 75-μm sections. The tissue sections were blocked and incubated for 30 min at room temperature, followed by incubation overnight at 4 °C in primary antibody anti-ALDH2 (1:200 dilution; Huata Biological Technology Co., LTD, Guangzhou, Guangdong, China), anti-caspase-3 (1:1000; Biogood Technology, Inc, Wuhan, Hubei, China) at a dilution, and HRP-conjugated second antibody for 1 h at 37 °C. Liquid diaminobenzidine was used as a chromogenic agent for 5 min, and sections were counterstained with Mayer's hematoxylin. PBS buffer was substituted for the first antibody as the negative control.

(TdT)-mediated biotin-16-dUTP nick-end labeling (TUNEL) assays

Paraffin sections were deparaffinized into water and covered with proteinase K solution for 15 min at room temperature. After destroying cell membrane, a proper volume of TUNEL kit agent 1 (TdT) and agent 2 (dUTP), at a ratio of 1:9 (v/v), was used to cover cells in a humidified box at 37 °C for 60 min. Then, the slides were shifted to methyl alcohol with 3% H_2O_2 and protected from light for 20 min. After drying, each section was placed in proper agent 3 (converter POD) to cover tissues in a humidified box at 37 °C for 30 min. Diaminobenzidine was used as a substrate to visualize positions of the proteins. Positive staining appeared brown in color. Nuclei were stained with hematoxylin.

FCM analyzed apoptosis

The cells were digested with trypsin and centrifuged at 1000 *g* for 5 min. The supernatants were removed, and the pellets were washed with phosphate-buffered solution (PBS). Approximately 5–10 × 10^4 cells were resuspended with 5 μl of Annexin V-FITC at room temperature for 10 min, which were collected by centrifugation. In the end, 10 μl of propidium iodide (PI) was added for 20 min and the samples were analyzed by FCM; FITC has green fluorescence and PI has red fluorescence.

Human 4-hydroxynonenal (HNE) ELISA detection

One hundred microliter of standard sample per well was added, covered with the adhesive strip provided, and incubated for 2 h at 37 °C. One hundred microliter of biotin antibody (1x) was added to each well, covered with a new adhesive strip, incubated for 1 h at 37 °C, and washed by filling each well with wash buffer (200 μl) using a squirt bottle, multichannel pipette, manifold dispenser, or auto washer, and leave it there for 2 min. One hundred microliter of HRP–avidin (1x) was added to each well and covered the microtiter plate with a new adhesive strip, and incubated for 1 h at 37 °C. Ninety microliter of TMB substrate was added to each well, incubated for 15–30 min at 37 °C, and protected it from light; 50 μl of stop solution was added to each well, gently tapped the plate to ensure thorough mixing. The optical density of each well was

determined within 5 min, using a microplate reader set to 450 nm.

Statistical analysis

Statistical analysis was performed with SPSS for WINDOWS (version 17.0; SPSS, Inc., Chicago, IL, USA). Continuous variables were presented as the mean ± standard deviation unless explicitly noted otherwise and analyzed with *t*-tests. Categorical variables were presented as absolute numbers and percentages and analyzed by a chi-square test. Two-sided *P*-values < 0.05 indicated statistical significance.

Results

Western blot and immunohistochemistry determined that expression of phosphorylated ALDH2 levels significantly decreased with the length of DBD time

Western blot analysis was used to validate the changes of phosphorylated ALDH2 in different times. Phosphorylated ALDH2 levels significantly decreased with the extending of DBD time, when compared with the sham ($P < 0.05$) (Fig. 1a and b). Furthermore, the levels of phosphorylated ALDH2 were significantly higher in DBD group when compared with those of sham rabbits at the same time ($P < 0.05$) (Fig. 1a and b). We determined changes in phosphorylated ALDH2 with time and locations in tissues, as shown in Fig. 1b, and ALDH2 was primarily located in endothelial cells. Data were mean ± SEM ($n = 10$).

TUNEL assay detected that apoptosis significantly increased with the extending of DBD time

Cellular apoptosis was determined by TUNEL assay. In the DBD group, the rates of cell apoptosis significantly increased with time ($P < 0.05$) (Fig. 2a), DBD 2 h 5.75% ± 1.04%, DBD 6 h 11.51% ± 2.18%, DBD 8 h 14.49% ± 2.81%. More importantly, DBD rabbits had higher apoptosis rates than the sham rabbits at the same time ($P < 0.05$) (Fig. 2a), sham 2 h 1.61% ± 0.23%, sham 6 h 2.69% ± 0.38%, sham 8 h 3.42% ± 0.43%. Data were mean ± SEM ($n = 10$).

Immunohistochemistry and Western blot tested that expression of cleaved caspase-3 increased with the extending of DBD time

The expression of cleaved caspase-3 was analyzed by immunohistochemistry and Western blot. In DBD group, the rabbits expressing cleaved caspase-3 increased with time when compared with the sham ($P < 0.05$) (Fig. 2b and c).

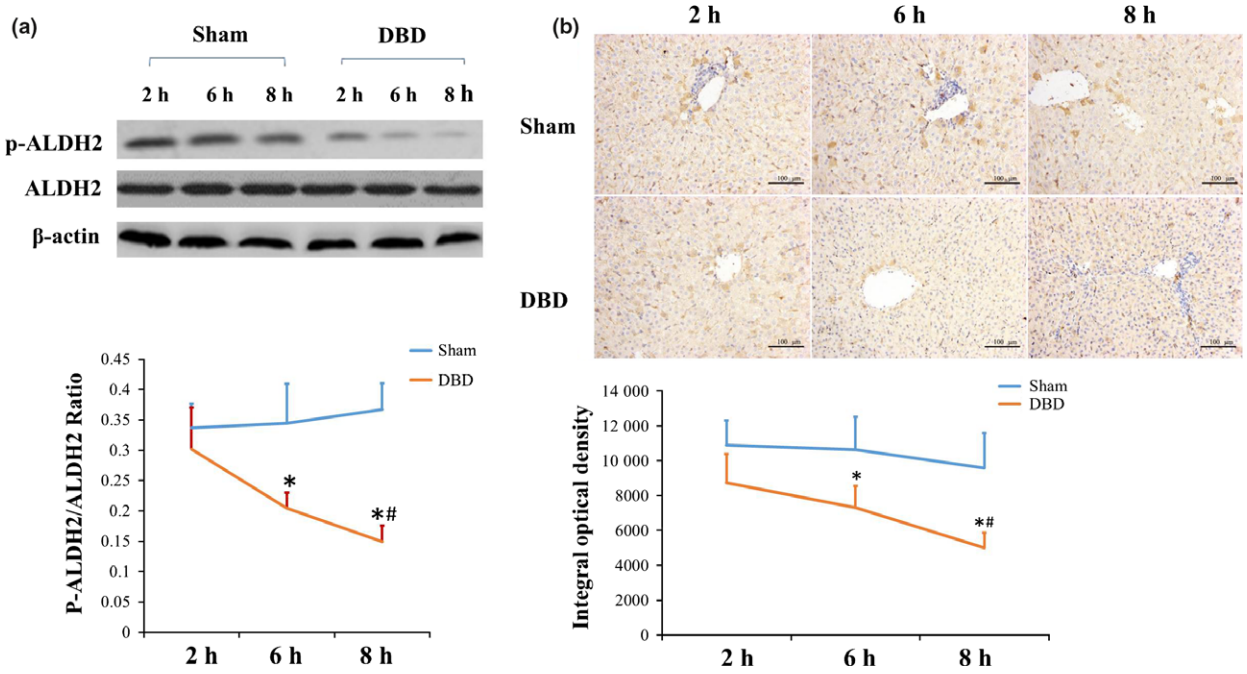

Figure 1 Expression of phosphorylated ALDH2 by Western blot and immunohistochemical testing between DBD and sham groups. In the DBD group, the levels of phosphorylated ALDH2 gradually reduced when compared with sham ($P < 0.05$) (Fig 1a and b). In comparison with the sham rabbits, the levels of phosphorylated ALDH2 were significantly lower in DBD group at the same time ($P < 0.05$) (Fig 1a and b). ALDH2 was primarily located in endothelial cells (Fig 1b). *$P < 0.05$, DBD group at 6 and 8 h compared with sham at 6 and 8 h; #$P < 0.05$, compared with the DBD rabbits at 2 and 6 h. Data were mean ± SEM ($n = 10$, magnification, ×200).

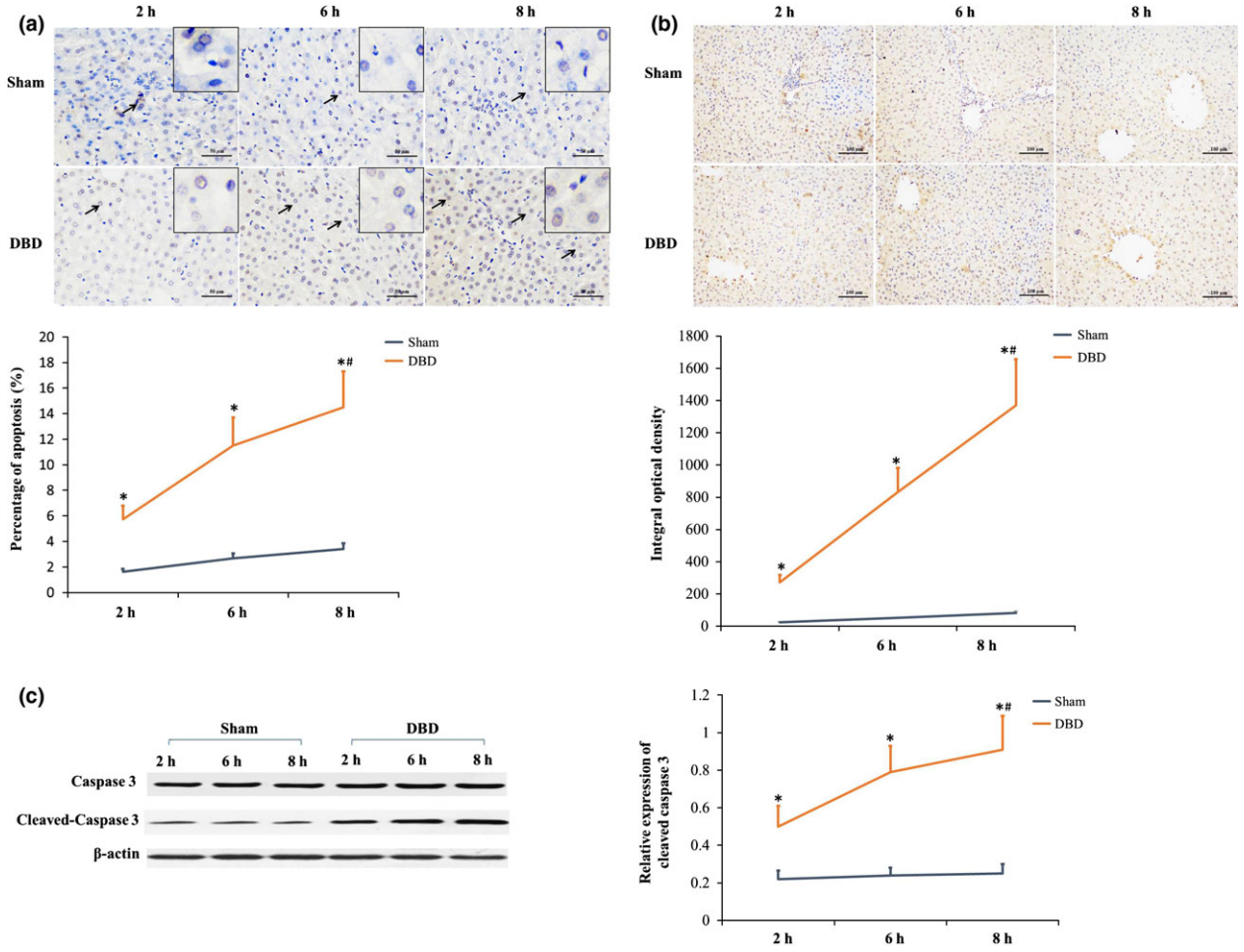

Figure 2 Apoptosis was detected by TUNEL assay, expression of cleaved caspase-3 by immunohistochemical testing, and Western blot between DBD and sham groups. TUNEL confirmed that DBD rabbits had higher apoptosis compared with sham rabbits ($P < 0.05$), and the rates of cell apoptosis in DBD groups significantly increased with time when compared with sham ($P < 0.05$) (Fig. 2a). *$P < 0.05$, DBD group at 2, 6, and 8 h compared with the sham at 2, 6, and 8 h; $^{\#}P < 0.05$, compared with the DBD rabbits at 2 and 6 h. Data are mean±SEM ($n = 10$, magnification, ×400). Apoptosis was showed with arrows (Fig. 2a). At the same time, in DBD group, the rabbits expressing cleaved caspase-3 increased with time when compared with sham ($P < 0.05$) (Fig. 2b and c). Furthermore, cleaved caspase-3 levels in the DBD group were higher than those in sham at the same time ($P < 0.05$) (Fig. 2b and c). *$P < 0.05$, DBD group at 2, 6, and 8 h compared with the sham at 2, 6, and 8 h; $^{\#}P < 0.05$, compared with the DBD rabbits at 2 and 6 h. Data were mean ± SEM ($n = 10$, magnification, ×200).

Furthermore, cleaved caspase-3 levels in the DBD group were higher than those of the sham at the same time ($P < 0.05$) (Fig. 2b and c). Data were mean±SEM ($n = 10$).

Western blot tested expression of ALDH2, bcl-2/bax ratio, and cleaved caspase-3 expression, ELISA detected accumulation of 4-HNE, and FCM analyzed cell apoptosis in HUVECs

As mentioned above, HUVECs were cultured under various conditions. As shown in Fig. 4a, hypoxia for 8 h (group 2) induced low expression of phosphorylated ALDH2 (Fig. 3a) and higher accumulation of 4-HNE (0.8068 ± 0.1540 ng/ml) ($P < 0.05$) (Fig. 3b). In contrast, the ALDH2 inhibitor, daidzein, plus hypoxia for 8 h (group 3) further decreased phosphorylated ALHD2 levels and increased accumulation of 4-HNE (1.8560 ± 0.2870 ng/ml) in cultured HUVECs ($P < 0.05$) (Fig. 3a and b). Culturing HUVECs in Alda-1 plus hypoxia (group 4) resulted in lower phosphorylated ALDH2 level and higher accumulation of 4-HNE (0.5830 ± 0.0890 ng/ml) than that in group 1, but higher phosphorylated ALDH2 level and lower accumulation of 4-HNE than that in group 2 ($P < 0.05$) (Fig. 3a and b). FCM was used to analyze cell apoptosis of HUVECs in different groups. The FCM assay indicated that the apoptosis rates of group 1 were 0.250% ± 0.129%. Based on the aforementioned

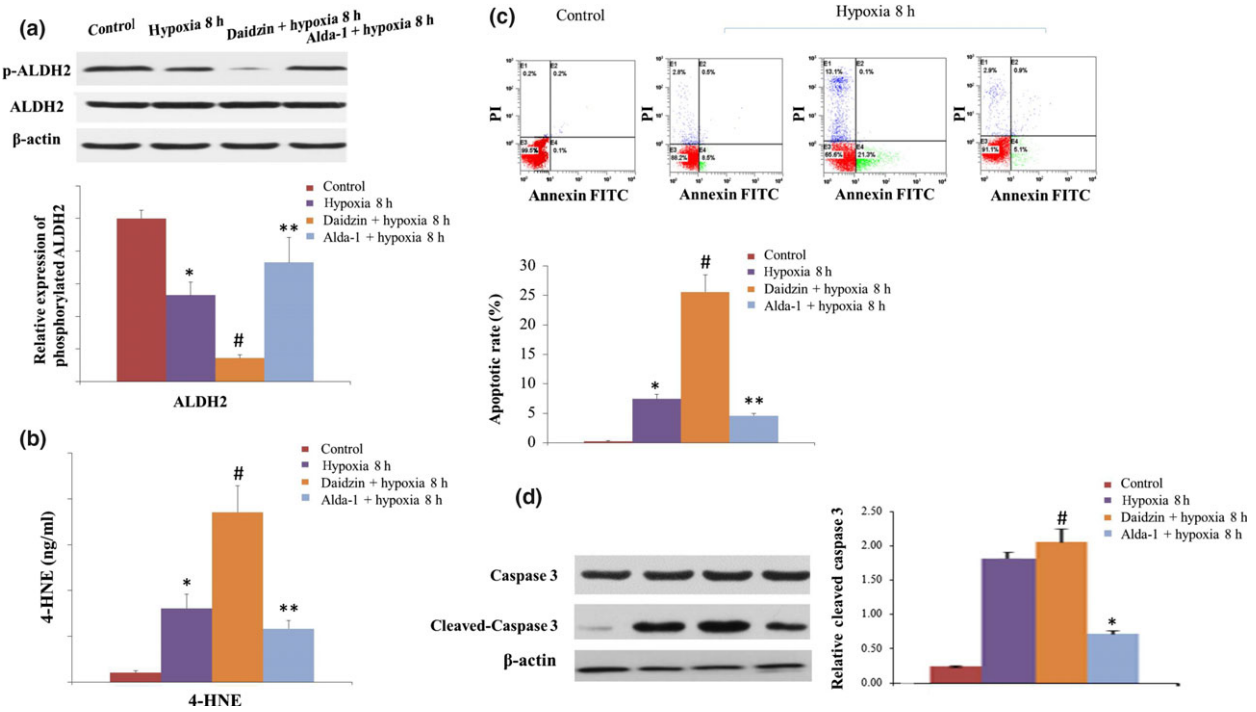

Figure 3 Expression of ALDH2 (Figure 3a), accumulation of 4-HNE (Figure 3b), cell apoptosis analysis (Figure 3c), and cleaved caspase-3 (Figure 3d) expression in HUVECs. The accumulation of 4-HNE, the apoptosis rates of HUVECs, and the expression of cleaved caspase-3 were higher after culturing in hypoxia compared with normal conditions ($P < 0.05$). The levels of 4-HNE, cleaved caspase-3, and apoptosis rates decreased when treated with Alda-1 plus hypoxia. However, daidzein plus hypoxia resulted in a higher accumulation of 4-HNE, apoptosis rates of HUVECs, and expression of cleaved caspase-3 than those in culture with hypoxia. *$P < 0.05$, hypoxia 8 h group compared with the other three groups. **$P < 0.05$, Alda-1+ hypoxia 8 h group compared with the other three groups. $^{\#}P < 0.05$, daidzein+ hypoxia 8 h group compared with the other three groups. Data were mean ± SEM ($n = 6$).

methods, the apoptosis rates of HUVECs were detected by FCM with significant differences at 8 h (group 2: 7.450% ± 0.755%, group 3: 25.60% ± 2.877%, and group 4: 4.575% ± 0.411%, $P < 0.05$) (Fig. 3c). The expression of cleaved caspase-3 was significantly higher in group 2 when compared with group 1 ($P < 0.05$) (Fig. 3d). Group 4 had a lower expression of cleaved caspase-3 than that in group 2, and group 3 had a higher expression of cleaved caspase-3 than that in group 2 ($P < 0.05$) (Fig. 3d). And meanwhile, incubation with adenovirus empty vector (10^6pfu/ml) plus hypoxia for 8 h (group 7) still kept the same levels of phosphorylated ALHD2 and the same ratio of bcl-2/bax as that in group 6 ($P > 0.05$). Culturing HUVECs with ad-ALDH2 (10^6pfu/ml) plus hypoxia (group 8) resulted in higher phosphorylated ALDH2 level and bcl-2/bax ratio than that in group 6 ($P < 0.05$) (Fig. 4). Data were mean±SEM ($n = 6$).

Western blot tested expression of P-P38, P-ERK, and P-JNK in HUVECs

We also studied on the role of ALDH2 involved in the MAPK pathway. Hypoxia for 8 h (groups 2 and 6) induced higher expression of P-P38, P-ERK, and P-JNK than that in groups 1 and 5, respectively ($P < 0.05$) (Fig. 5a and b). Culturing HUVECs in the ALDH2 inhibitor, daidzein, plus hypoxia and ischemia for 8 h (group 3) increased P-JNK ($P < 0.05$) (Fig. 5a), but there were no differences between P-P38 and P-ERK. Culturing HUVECs in Alda-1 plus hypoxia (group 4) resulted in lower levels of P-P38, P-ERK, and P-JNK than that in group 1, and higher levels than that in group 2 ($P < 0.05$) (Fig. 5a), which was the same case in group 8 ($P < 0.05$) (Fig. 5b). Data were mean±SEM ($n = 6$).

Discussion

Previously, we established a rabbit DBD model to study on the liver morphology and found no obvious changes at different time points. We subsequently utilized a proteomic assay to screen differentiated proteins in the liver to determine whether there are any differences notable in DBD livers. As a result, ALDH2, one of the differential proteins, was screened by our group and shown to have lower levels in brain-dead rabbits than that in the sham group [12,13]. In the present study, we determined the ALDH2 levels

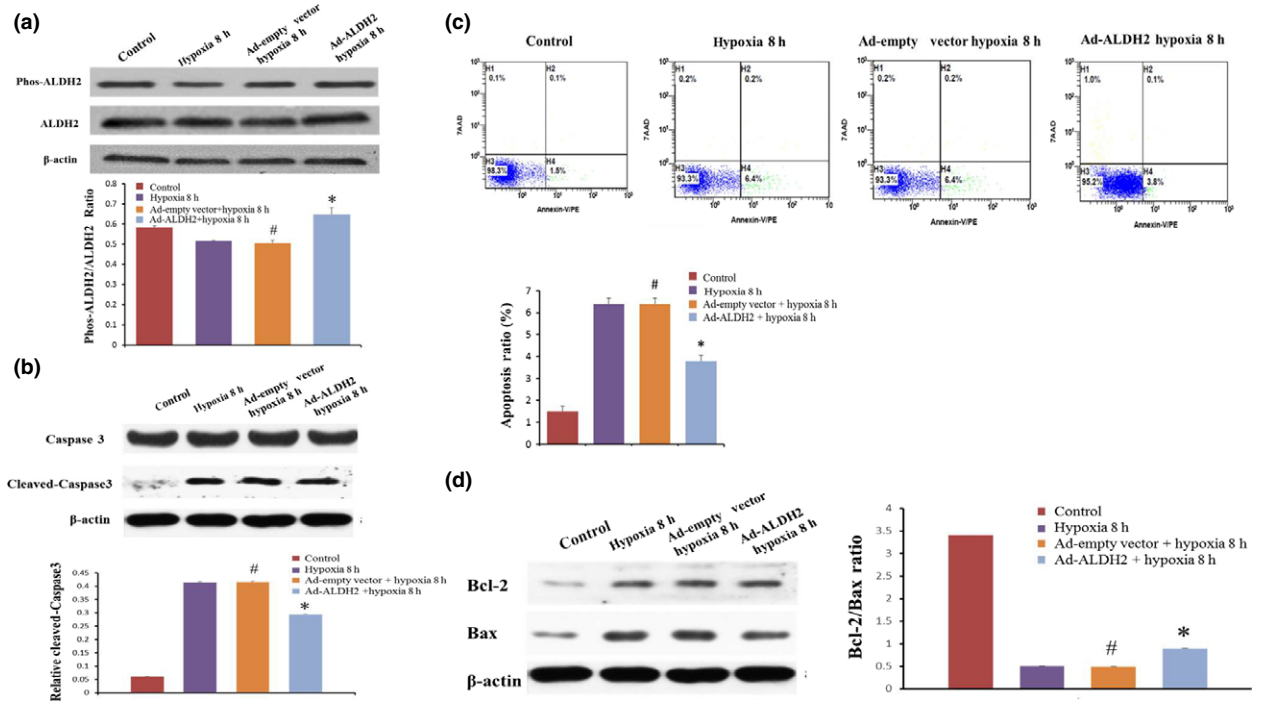

Figure 4 Expression of ALDH2 (Figure 4a), cell apoptosis analysis (Figure 4c), and cleaved caspase-3 (Figure 4b), bcl-2, and bax expression (Figure 4d) in HUVECs. The bcl-2/bax ratio was significantly lower, and the apoptosis rates of HUVECs and the expression of cleaved caspase-3 were higher after cultured with hypoxia compared with normal conditions ($P < 0.05$). In the ad-ALDH2 group, overexpressed ALDH2 plus hypoxia resulted in a higher bcl-2/bax ratio, lower apoptosis rates of HUVECs, and lower expression of cleaved caspase-3 than those in culture with hypoxia. $^{*}P < 0.05$, ad-ALDH2 + hypoxia 8 h group compared with the other three groups. $^{\#}P > 0.05$, ad-empty vector hypoxia 8 h group compared with the hypoxia 8 h group. Data were mean ± SEM ($n = 6$).

by Western blot analysis, and results indicated that phosphorylated ALDH2 levels gradually decreased with time after brain death, which was consistent with previous findings identified by mass spectrometry [12,13]. Several reports had revealed that ALDH2 levels also decreased gradually in other circumstances [23,24].

A study had shown that ALDH2 antagonizes damages to nerves and endothelial cells caused by oxidative stress [25]. The high expression of the ALDH2 gene could protect cells against the toxicity of chemical substances *in vitro* and also protect against apoptosis through resistance to oxidative stress [26]. Based on these studies, there is a hypothesis that brain death could suppress the expression of ALDH2 in liver tissue, which could weaken the ability of ALDH2 to resist hepatocyte apoptosis, leading to increased liver damage. The overexpression of ALDH2 attenuates apoptosis caused by chronic alcohol exposure [15]. In contrast, the upregulation of ALDH2 played a role in the inhibition of apoptosis and protection of hepatic cells [17]; therefore, we postulated that there were relationships between ALDH2 and apoptosis. The TUNEL assay and expression of caspase-3 showed that the apoptosis rates and levels of cleaved caspase-3 increased significantly. We found that brain death resulted in decreased ALDH2 and increased hepatocyte apoptosis. However, the molecular mechanism underlying ALDH2 and brain death had yet to be elucidated in its entirety.

Immunohistochemistry further proved that phosphorylated ALDH2 was mostly expressed in the endothelium cells. To explore the role of phosphorylated ALDH2 in regulating apoptosis and mechanisms of hepatic injury, we developed a hypoxia model of HUVECs to simulate brain death. In our study, the apoptosis rates of HUVECs after culturing in hypoxic conditions for 8 h were significantly higher than those in controls. The ALDH2 inhibitor plus hypoxia further improved the apoptosis rates; thus, the downregulation of ALDH2 had a role in promoting cell apoptosis and destroying hepatic cells. On the other hand, the activator of ALDH2 (Alda-1) in the presence of hypoxia partially reduced apoptosis, and incubation HUVECs with ad-ALDH2 (10^6pfu/ml) plus hypoxia significantly alleviated the apoptosis. It seemed that Alda-1 decreased apoptosis which might contribute to enhanced quality of liver donors.

Based on previous studies, the most prominent pathologic changes were low blood perfusion flow dynamics and local hypoxia in hepatic tissues during brain death. Loss of

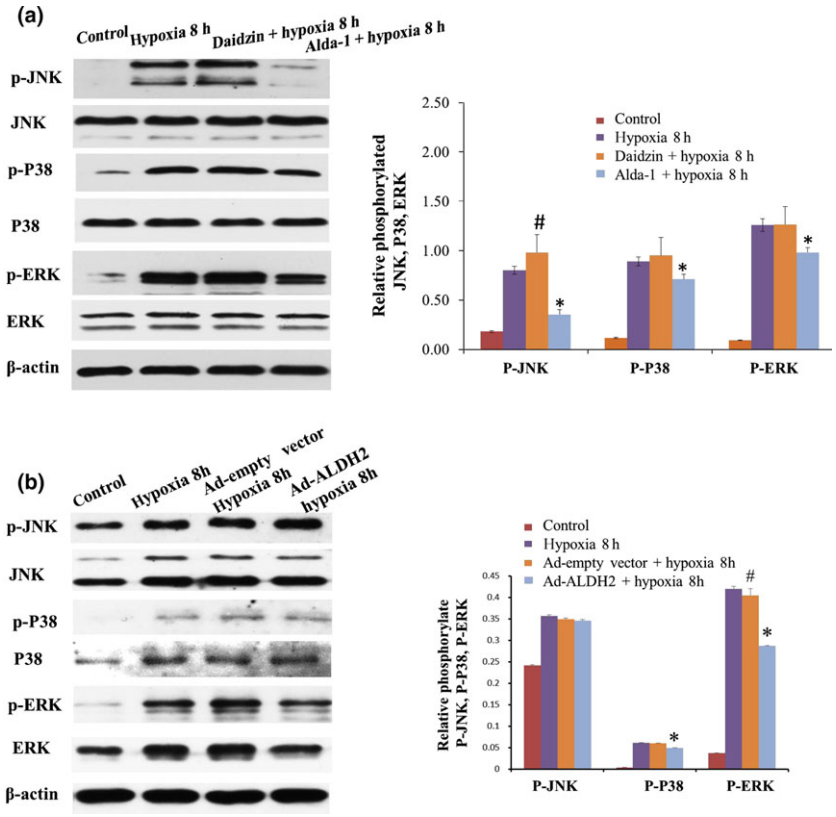

Figure 5 Expression of P-JNK, P-P38, and P-ERK by Western blot between hypoxia and ischemia groups in HUVECs. Hypoxia-increased P-JNK, P-P38, and P-ERK were significantly higher than those in controls ($P < 0.05$). Alda-1 plus hypoxia led to P-JNK, P-P38, and P-ERK lower than that in hypoxia groups. Daidzein plus hypoxia led to P-JNK higher than that in hypoxia groups, but there were no differences in P-P38 and P-ERK. *$P < 0.05$, Alda-1+ hypoxia 8 h group compared with the other three groups. $^{\#}P < 0.05$, daidzein+ hypoxia 8 h group compared with the other three groups. Data were mean ± SEM ($n = 6$) (Fig. 5a). The ad-ALDH2 group which overexpressed ALDH2 plus hypoxia led to P-P38, and P-ERK lower than that in hypoxia groups. At the same time, there were no differences in ad-empty vector hypoxia 8 h group and hypoxia 8 h group. *$P < 0.05$, ad-ALDH2+ hypoxia 8 h group compared with the other three groups. $^{\#}P > 0.05$, ad-empty vector hypoxia 8 h group compared with the hypoxia 8 h group. Data were mean ± SEM ($n = 6$) (Fig. 5b).

mitochondrial function arose from excessive accumulation of oxidative stress [27,28]. In addition, reactive oxygen species were oversynthesized by inner cells and induced oxidative stress [29,30]. MAPK was noted to be one of the downstream effectors. The activation of MAPK resulted in the upregulation of inflammatory factors [31,32]. The inflammatory reactions activated oxidative stress-sensitive hepatic cells. In contrast, local inflammatory infiltration also damaged astrocytes, endothelial cells, and hepatic cells, which further harmed liver function and structure [33,34]. Eventually, all of these factors led to a poor quality of liver donors.

To explore the role of ALDH2 in regulating apoptosis through MAPK pathway, our data demonstrated that the levels of 4-HNE, P-P38, P-ERK, P-JNK, and cleaved caspase-3 in the hypoxia groups were significantly higher with hypoxia for 8 h. Daidzein plus hypoxia resulted in elevated 4-HNE, P-P38, P-ERK, P-JNK, and cleaved caspase-3 levels after culturing cells for 8 h. When Alda-1 was combined with hypoxia, the expression of 4-HNE, P-P38, P-ERK, P-JNK, and cleaved caspase-3 was weakened, higher than that in controls, but lower than that in hypoxia groups. Hence, the downexpression of ALDH2 accumulated 4-HNE, and then, 4-HNE could activate the MAPK signaling pathway and promoted cell apoptosis. Furthermore, the overexpression of ALDH2 decreased 4-HNE, inhibited the MAPK signaling pathway, and decreased apoptosis.

In conclusion, we found low expression of ALDH2 and high rates of apoptosis in the livers of donor brain-dead rabbits. Furthermore, decreased ALDH2 led to apoptosis in HUVECs through MAPK pathway.

Research highlights

1. Phosphorylated ALDH2 levels significantly decreased with the length of DBD time

2. Apoptosis significantly increased with the extending of DBD time
3. Decreased ALDH2 led to apoptosis in hypoxic HUVECs
4. MAPK pathway was involved in hypoxic HUVECs

Authorship

ZZ and SY: designed and performed the research, analyzed the data, and wrote the article. YX and LW: performed the research, contributed ideas, and helped write the article. XF, LL, FZ, MZ and XY: helped establish the model in vivo. HW and MC: helped the experiment in vitro. DSCK and WH: provided guidance and revised the article. YW and QY: designed the experiments, provided overall guidance, and helped with the manuscript.

Funding

This work was supported by The State Key Program of National Natural Science of China, No: 21334005; Science and Technology Projects of Wuhan City, No: 2013060 705010326; 2013060602010247; and The Fundamental Research Funds for the Central Universities.

Acknowledgements

The authors are grateful to Prof. Yi Zhang and Guizhu Peng (Institute of Hepatobiliary Diseases of Wuhan University, China) in revising the manuscript.

References

1. Olson JC, Wendon JA, Kramer DJ, *et al.* Intensive care of the patient with cirrhosis. *Hepatology* 2011; **54**: 1864–1872.
2. Huang J, Millis JM, Mao Y, Millis MA, Sang X, Zhong S. A pilot programme of organ donation after cardiac death in China. *Lancet* 2012; **379**: 862–865.
3. Huang J, Wang H, Fan ST, *et al.* The national program for deceased organ donation in China. *Transplantation* 2013; **96**: 5–9.
4. Zhong Z, Ye Q, Fan L, *et al.* Effect of machine perfusion on preservation of kidneys from donors after cardiac death. *Chinese J Transplant* 2013; **7**: 1–5.
5. Chinese Society of Organ Transplantation, Chinese Medical Association. National guidelines for donation after cardiac death in China. *Hepatobiliary Pancreat Dis Int* 2013; **12**: 234–238.
6. Sam R, Leehey DJ. Improved graft survival after renal transplantation in the United States, 1988 to 1996. *N Engl J Med* 2000; **342**: 1837–1838.
7. Terasaki PI, Cecka JM, Gjertson DW, Takemoto S. High survival rates of kidney transplants from spousal and living unrelated donors. *N Engl J Med* 1995; **333**: 333–336.
8. Adrie C, Monchi M, Fulgencio JP, *et al.* Immune status and apoptosis activation during brain death. *Shock* 2010; **33**: 353–362.
9. Van Der Hoeven JA, Moshage H, Schuurs T, Nijboer M, Van Schilfgaarde R, Ploeg RJ. Brain death induces apoptosis in donor liver of the rat. *Transplantation* 2003; **76**: 1150–1154.
10. Klein AS, Messersmith EE, Ratner LE, Kochik R, Baliga PK, Ojo AO. Organ donation and utilization in the United States, 1999–2008. *Am J Transplant* 2010; **10**: 973–986.
11. Lin H, Okamoto R, Yamamoto Y, *et al.* Hepatic tolerance to hypotension as assessed by the changes in arterial ketone body ratio in the state of brain death. *Transplantation* 1989; **47**: 444–448.
12. Zhong Z, Ye Q, Wang Y, Li L, Fan X. Detection and identification of aldehyde dehydrogenase as an indicator in the assessment of liver quality of rabbits with brain death. *Chinese J Hepatobiliary Surg* 2013; **7**: 534–538.
13. Du B, Li L, Zhong Z, *et al.* Brain death induces the alteration of liver protein expression profiles in rabbits. *Int J Mol Med* 2014; **34**: 578–84.
14. Sun L, Ferreira JC, Mochly-Rosen D. ALDH2 activator inhibits increased myocardial infarction injury by nitroglycerin tolerance. *Sci Transl Med* 2011; **3**: 107ra11.
15. Xu D, Guthrie JR, Mabry S, Sack TM, Truog WE. Mitochondrial aldehyde dehydrogenase attenuates hyperoxia-induced cell death through activation of ERK/MAPK and PI3K-Akt pathways in lung epithelial cells. *Am J Physiol Lung Cell Mol Physiol* 2006; **291**: L966–975.
16. Guo R, Zhong L, Ren J. Overexpression of ALDH2 attenuates chronic alcohol exposure-induced apoptosis, change in Akt and Pim signaling in liver. *Clin Exp Pharmacol Physiol* 2009; **36**: 463–468.
17. Chen T, Cui J, Liang Y, *et al.* Identification of human liver mitochondrial aldehyde dehydrogenase as a potential target for microcystin-LR. *Toxicology* 2006; **220**: 71–80.
18. Li SY, Li Q, Shen JJ, *et al.* Attenuation of acetaldehyde-induced cell injury by overexpression of aldehyde dehydrogenase-2 (ALDH2) transgene in human cardiac myocytes: role of MAP kinase signaling. *J Mol Cell Cardiol* 2006; **40**: 283–294.
19. Lin MH, Yen JH, Weng CY, Wang L, Ha CL, Wu MJ. Lipid peroxidation end product 4-hydroxy-trans-2-nonenal triggers unfolded protein response and heme oxygenase-1 expression in PC12 cells: roles of ROS and MAPK pathways. *Toxicology* 2014; **315**: 24–37.
20. Quality Standards Subcommittee of the American Academy of Neurology. Practice parameters for determining brain death in adults (Summary statement). *Neurology* 1995; **45**: 1012–1014.
21. Zhang P, Xu D, Wang S, *et al.* Inhibition of aldehyde dehydrogenase 2 activity enhances antimycin-induced rat cardiomyocytes apoptosis through activation of MAPK signaling pathway. *Biomed Pharmacother* 2011; **65**: 590–593.

22. Chen CH, Budas GR, Churchill EN, Disatnik MH, Hurley TD, Mochly-Rosen D. Activation of aldehyde dehydrogenase-2 reduces ischemic damage to the heart. *Science* 2008; **321**: 1493–1495.
23. Lang XE, Wang X, Zhang KR, Lv JY, Jin JH, Li QS. Isoflurane preconditioning confers cardioprotection by activation of ALDH2. *PLoS ONE* 2013; **8**: e52469.
24. Solito R, Corti F, Chen CH, *et al.* Mitochondrial aldehyde dehydrogenase-2 activation prevents beta-amyloid-induced endothelial cell dysfunction and restores angiogenesis. *J Cell Sci* 2013; **126**: 1952–1961.
25. Murphy TC, Arntzen R, Picklo MJ Sr. Nitrate-based vasodilators inhibit multiple vascular aldehyde dehydrogenases. *Cardiovasc Toxicol* 2005; **5**: 321–332.
26. Churchill EN, Disatnik MH, Mochly-Rosen D. Time-dependent and ethanol-induced cardiac protection from ischemia mediated by mitochondrial translocation of varepsilon PKC and activation of aldehyde dehydrogenase 2. *J Mol Cell Cardiol* 2009; **46**: 278–284.
27. Lucas DT, Szweda LI. Cardiac reperfusion injury: aging, lipid peroxidation, and mitochondrial dysfunction. *Proc Natl Acad Sci USA* 1998; **95**: 510–514.
28. Costa AD, Pierre SV, Cohen MV, Downey JM, Garlid KD. cGMP signalling in pre- and post-conditioning: the role of mitochondria. *Cardiovasc Res* 2008; **77**: 344–352.
29. Lagranha CJ, Deschamps A, Aponte A, Steenbergen C, Murphy E. Sex differences in the phosphorylation of mitochondrial proteins result in reduced production of reactive oxygen species and cardioprotection in females. *Circ Res* 2010; **106**: 1681–1691.
30. Endo J, Sano M, Katayama T, *et al.* Metabolic remodeling induced by mitochondrial aldehyde stress stimulates tolerance to oxidative stress in the heart. *Circ Res* 2009; **105**: 1118–1127.
31. Mandrekar P, Szabo G. Signalling pathways in alcohol-induced liver inflammation. *J Hepatol* 2009; **50**: 1258–1266.
32. Qi D, Hu X, Wu X, *et al.* Cardiac macrophage migration inhibitory factor inhibits JNK pathway activation and injury during ischemia/reperfusion. *J Clin Investig* 2009; **119**: 3807–3816.
33. Miki C, Gunson BK, Buckels JA, Uchida K, Mohri Y, Kusunoki M. Methylprednisolone therapy in deceased donors reduces inflammation in the donor liver and improves outcome after liver transplantation. *Ann Surg* 2009; **250**: 502–503; author reply 3–4.
34. Hoffmann MW, Wonigeit K, Steinhoff G, Herzbeck H, Flad HD, Pichlmayr R. Production of cytokines (TNF-alpha, IL-1-beta) and endothelial cell activation in human liver allograft rejection. *Transplantation* 1993; **55**: 329–335.